The American Journal of Pathology, Vol. 178, No. 2, February 2011

DOI: 10.1016/j.ajpath.2010.10.009

Cardiovascular, Pulmonary, and Renal Pathology

Basigin/CD147 Promotes Renal Fibrosis after Unilateral Ureteral Obstruction

Noritoshi Kato,*† Tomoki Kosugi,*† Waichi Sato,† Takuji Ishimoto,† Hiroshi Kojima,† Yuka Sato,† Kazuma Sakamoto,* Shoichi Maruyama,† Yukio Yuzawa,† Seiichi Matsuo,† and Kenji Kadomatsu*

From the Departments of Biochemistry and Nephrology of Internal Medicine,† Nagoya University Graduate School of Medicine, Nagoya, Japan*

Regardless of their primary causes, progressive renal fibrosis and tubular atrophy are the main predictors of progression to end-stage renal disease. Basigin/CD147 is a multifunctional molecule–it induces matrix metalloproteinases and hyaluronan, for example–and has been implicated in organ fibrosis. However, the relationship between basigin and organ fibrosis has been poorly studied. We investigated basigin's role in renal fibrosis using a unilateral ureteral obstruction model. Basigin-deficient mice ($Bsg^{-/-}$) demonstrated significantly less fibrosis after surgery than $Bsg^{+/+}$ mice. Fewer macrophages had infiltrated in $Bsg^{-/-}$ kidneys. Consistent with these *in vivo* data, primary cultured tubular epithelial cells from $Bsg^{-/-}$ mice produced less matrix metalloproteinase and exhibited less motility on stimulation with transforming growth factor β. Furthermore, $Bsg^{-/-}$ embryonic fibro blasts produced less hyaluronan and α-smooth muscle actin after transforming growth factor β stimulation. Together, these results demonstrate for the first time that basigin is a key regulator of renal fibrosis. Basigin could be a candidate target molecule for the prevention of organ fibrosis. *(Am J Pathol 2011, 178:572–579; DOI: 10.1016/j.ajpath.2010.10.009)*

Regardless of the primary disease process, renal interstitial fibrosis is the key determinant of chronically diseased kidney and the main prognostic predictor of renal function.[1] Excessive accumulation of extracellular matrix (ECM) leads to dysfunction of the organ and state of fibrosis.[2] ECM turnover is regulated by the activity of matrix metalloproteinases (MMPs). Although transforming growth factor β (TGF-β) stimulates α-SMA expression as well as ECM production by fibroblasts, it also regulates the expression of MMPs.[3,4] Conversely, some MMPs, such as MMP-2, MMP-9, and MT1-MMP, activate latent TGF-β.[5,6] Therefore, ECM synthesis and degradation are intricately regulated by TGF-β, MMPs, and others. In this context, it should also be noted that hyaluronan plays a crucial role in the TGF-β–driven differentiation of fibroblasts into myofibroblasts.[7–10] Endogenous hyaluronan is necessary for fibroblast differentiation and maintenance of the myofibroblast phenotype through autocrine TGF-β action.[11]

Basigin (Bsg)/CD147 (*Bsg* is the name of the mouse gene) is a glycosylated transmembrane protein that belongs to the immunoglobulin superfamily. It is expressed by many types of cells, including hematopoietic, epithelial, endothelial, and tumor cells.[12,13] It is well documented that Bsg induces MMPs, so it is also known as an extracellular matrix metalloproteinase inducer (EMMPRIN).[14] It is highly up-regulated in many malignant cancer cells and is thought to contribute to cell survival, invasion, metastasis, and multidrug resistance.[15] Studies targeting Bsg to prevent tumor growth using RNAi techniques have achieved successful outcomes.[16–19] Along with MMPs, Bsg is also involved in the production of vascular endothelial growth factor and hyaluronan.[20–24] Bsg interacts with a wide range of binding partners.[25] For example, it binds to caveolin, cyclophilin, monocarboxylate transporter, and Bsg itself.[26–29] Through the interaction with monocarboxylate transporter, Bsg plays a role in lactate metabolism. Furthermore, Bsg promotes the differentiation of fibroblasts into myofibroblasts by inducing α-SMA expression in corneal fibroblasts.[30]

We previously generated Bsg-deficient mice ($Bsg^{-/-}$) and reported several abnormalities, including male and female sterility, progressive retinal degeneration, increased cell proliferation on mixed lymphocyte culture, decreased

Supported by Grants-in-Aid from the Ministry of Education, Culture, Sports, Science, and Technology of Japan (the global COE program to Nagoya University).

Accepted for publication October 1, 2010.

N.K. and T.K. contributed equally to this work.

Address reprint requests to Kenji Kadomatsu, M.D., Ph.D., Department of Biochemistry, Nagoya University Graduate School of Medicine, 65 Tsurumai-cho, Showa-ku, Nagoya 466-8550, Japan. E-mail: kkadoma@med.nagoya-u.ac.jp.

memory function, and abnormal sensory function.[31–33] Most recently, we also found that Bsg is an E-selectin ligand and is involved in renal ischemia/reperfusion injury.[34]

In this study, we focused on Bsg functions in renal fibrosis induced by unilateral ureteral obstruction (UUO). Bsg orchestrates renal fibrosis formation through MMPs, hyaluronan production, and macrophage infiltration. To the best of our knowledge, this is the first report on the critical role of Bsg in renal fibrosis.

Materials and Methods

Animals and Experimental Design

Mice deficient in *Bsg* were generated as described previously.[35] Because $Bsg^{-/-}$ mice were hardly born through ordinary mating, we established the following protocol. $Bsg^{+/-}$ mice with 129/SV background were backcrossed with C57BL/6J mice to produce F1 hybrid offspring (reverse F1 hybrid). By intercrossing these mice, mixed reverse F2 mice were generated, and were used in this study. All experiments were performed with $Bsg^{+/+}$ and $Bsg^{-/-}$ littermates. We used 96 mice (48 mice in each genotype, respectively), which were 8- to 12-week-old males weighing 20 to 25 g. These mice were divided into seven groups at each time point ($n = 8$/each group on day 0, 7, and 14; $n = 6$/each group on day 1, 2, 3, and 5, respectively). The mice were housed under controlled environmental conditions and maintained with standard food and water.

In $Bsg^{+/+}$ and $Bsg^{-/-}$ mice sedated by general anesthesia, an incision was made in the right side of the back, and complete ureteral obstruction was performed by double-ligating the right ureter using 4-0 silk. Sham-operated mice had their ureters exposed but not ligated. Mice were sacrificed at different time points as indicated after surgery. Kidneys were removed for examination. Blood and urine samples were collected on the day of sacrifice. Kidney tissues were processed for histology and protein extraction. All of the animal experiments were performed in accordance with the animal experimentation guidelines of Nagoya University School of Medicine.

Histology

The removed kidneys were fixed in 4% paraformaldehyde, embedded in paraffin, and then cut into 4-μm sections. The sections were stained with polyclonal goat anti-human type III collagen (Southern Biotech, Birmingham, AL) and polyclonal goat anti-mouse Bsg (R&D Systems, Minneapolis, MN) followed by detection with biotin-conjugated rabbit anti-goat IgG (Nichirei, Tokyo, Japan). Immunostaining was performed by the streptavidin (Chemicon International, Temecula, CA) -biotin immunoperoxidase method. The staining was visualized with 3,3′-diaminobenzidine (Dako, Carpinteria, CA), a brown color being produced. Negative controls involved replacement of the primary antibodies with species-matched antibodies.

The sections were stained with periodic acid-Schiff reagent (PAS). Tubular dilation was assessed by counting the number of dilated tubules in the cortex of each section.[36] They were also stained with a terminal deoxynucleotidyl transferase-mediated dUTP nick-end labeling (TUNEL) assay kit according to the manufacturer's instructions (Roche Applied Science, Indianapolis, IN). The number of apoptotic cells was examined in the cortex of each section.

Parts of the kidney tissues were snap-frozen in liquid nitrogen. Sections (2-μm thick) were cut with a cryostat and then fixed in acetone. The cryosections were stained with rat anti-mouse monocyte-macrophage marker F4/80 (Serotec, Oxford, UK) followed by detection with fluorescein isothiocyanate rabbit anti-rat IgG (Zymed Laboratories, San Francisco, CA). Macrophages positive for F4/80 were counted by examining 10 fields of the cortex under a microscope at $\times$200 magnification in a blind manner.

Real-Time PCR

Mouse kidney tissues were snap-frozen in liquid nitrogen for total mRNA isolation. To perform mRNA extraction and cDNA synthesis, we used the RNeasy Mini Kit and QuantiTect Reverse Transcriptional Kit (Qiagen, Hilden, Germany) according to the manufacturer's instructions. Real-time PCR analysis was performed with an Applied Biosystems Prism 7500HT sequence detection system using TaqMan gene expression assays according to the manufacturer's specifications (Applied Biosystems, Foster City, CA). TaqMan probes and primers for type III collagen (Col3a1; Mm00802331_m1), TGF-β_1 (*Tgfb1*; Mm00441724_m1), hyaluronan synthase 2 (*Has2*; Mm00515089_m1), α-SMA (*Acta2*; Mm01546133_m1), β-actin (*Actb*; Mm00607939_s1), and glyceraldehyde-3-phosphate dehydrogenase (*Gapdh*; Mm99999915_g1) were used. Amplification data were analyzed with Applied Biosystems Sequence Detection software version 1.3.1.

Western Blot Analysis

Mouse kidney tissues were snap-frozen in liquid nitrogen for protein isolation and then lysed in radio-immunoprecipitation assay buffer (50 mmol/L Tris-HCl, 150 mmol/L NaCl, 1% Nonidet P, 1% deoxycolic acid, and 0.05% SDS). Western blot analysis was performed as described previously.[37]

Briefly, we separated the samples by 10% SDS-PAGE and then transferred them to a nitrocellulose membrane (Whatman, Florham Park, NJ). We blocked the membranes with 5% (w/v) dry fat-free milk in PBS with 0.1% Tween for 60 minutes at room temperature. The blots were subsequently incubated with goat anti-mouse Bsg antibody (R&D Systems), monoclonal anti-β actin antibody (Sigma Aldrich, St. Louis, MO), or rat anti-mouse E-selectin antibody (R&D Systems), followed by incubation with peroxidase-conjugated anti-goat IgG, rat IgG, and mouse IgG (Jackson Immunoresearch Laboratories, West Grove, PA). Proteins were visualized with an enhanced chemiluminescence detection system (Amersham Pharmacia, Amersham Biosciences, Piscataway, NJ). The density of each band was measured using the public domain National Institutes of Health image program.

Gelatin Zymography

Kidney tissue homogenates and cultured media of TECs were subjected to gelatin zymography of the MMP proteolytic activity. Gelatin zymography was performed using commercial kit (Invitrogen, Carlsbad, CA) according to the manufacturer's instructions. Briefly, the homogenates were loaded into 7.5% SDS-polyacrylamide gel containing 1 mg/ml gelatin. After electrophoresis, the gel was incubated in 2.5% Triton X-100 at room temperature for 30 minutes with gentle shaking and then at 37°C for 24 hours in a developing buffer containing $CaCl_2$ Tris-HCl. The gel was stained with Coomassie blue. Proteinase activity was detected as unstained bands on a blue background, representing areas of gelatin digestion. The density of each band was measured using the public-domain National Institutes of Health image program.

Cell Culture

Tubular epithelial cells (TECs) were isolated from the kidneys of adult $Bsg^{+/+}$ or $Bsg^{-/-}$ mice, as described previously.[38] Briefly, the renal cortex divided from the medulla was resolved with collagenase (Wako Chemicals, Miyazaki, Japan) and the lysate was then filtered through 38-μm strainer, using a mesh sieving method. The fluid was centrifuged to pellet the various renal cells, which were plated with cultured media for 1 hour of incubation. To avoid the contamination of mesangial cells and various cells, adherent cells were removed, and a supernatant solution including numerous TECs was incubated to another plate for 72 hours in K1 medium [224.25 ml Ham's F12; 226.25 ml Dulbecco's modified Eagle's medium (DMEM); and 12.5 ml HEPES] containing 10% fetal bovine serum (GIBCO BRL, Gaithersburg, MD) and hormones [epidermal growth factor (50 pg/ml); insulin-transferrin-sodium selenite media supplement (0.12 IU/ml), prostaglandin E_1 (1.25 ng/ml), hydrocortisone (18 ng/ml); T3 (34 pg/ml)]. The fourth and fifth passages were used for experiments. These cells isolated from the kidneys were determined to be of proximal tubular origin by means of immunofluorescence histochemistry; cells were stained positively for cytokeratin (ENZO Diagnostics, Farmingdale, NY); brush border vesicle (BBV; gift from Dr. G. Andres)[39]; desmin (Progen, Heidelberg, Germany), and Phalloidin (Invitrogen). These staining patterns were the same as those previously reported.[40]

Subconfluent tubular epithelial cells were incubated in serum-free medium for 24 hours to arrest and synchronize cell growth. After that, the medium was changed to fresh serum-free DMEM containing 5 ng/ml recombinant TGF-β (R&D Systems) for 0, 1, 3, 6, 12, and 24 hours in the time-course study. *The culture* medium was subjected to gelatin zymography.

Mouse embryonic fibroblast (MEF) was established from the embryos of $Bsg^{+/+}$ and $Bsg^{-/-}$ mice and then cultured in DMEM containing 10% fetal bovine serum.[41] After the cells were starved for 24 hours, the medium was changed to fresh serum-free DMEM containing 5 ng/ml recombinant TGF-β (R&D Systems). Cells were then used for the collection of mRNA, and culture medium was used for hyaluronan ELISA.

Cell Invasion Assay

To compare cell migration capacity between $Bsg^{+/+}$ TECs and $Bsg^{-/-}$, we used the Cultrex Cell Invasion/Migration Assay according to the manufacturer's instructions (Trevigen, Gaithersburg, MD) to mimic *in vivo* the tubular basement membrane microenvironment and the renal interstitium and to screen compounds that influence cellular digestion and migration across ECM. This assay used a simplified Boyden chamber design with an 8-micron polyethylene terephthalate membrane coated with basement membrane extract. The bottom wells of a 96-well Boyden chamber were filled with DMEM containing 5 ng/ml TGF-β (R&D Systems). $Bsg^{+/+}$ and $Bsg^{-/-}$ TECs were labeled with calcein-AM beforehand, and then 5.0×10^4 cells/well were added to the upper chamber. The Boyden chamber was incubated for 24 hours at 37°C to allow the possible migration of cells into the lower chamber. The number of migrated cells was estimated as fluorescence using Fluoroskan AscentCF (Labsystems, Helsinki, Finland).

Statistical Analysis

All values are expressed as means ± SD. Statistical analysis was performed with the unpaired, two-tailed Student's *t*-test for single comparisons. Values of $P < 0.05$ were considered to indicate statistically significant differences.

Results

$Bsg^{-/-}$ *Mice Have Less Tubulointerstitial Fibrosis*

To determine the role of Bsg in renal fibrosis, we subjected $Bsg^{+/+}$ and $Bsg^{-/-}$ mice to UUO surgery and compared the degrees of type III collagen deposition in the tubulointerstitium. At 7 days after UUO operation, both genotypes exhibited increased expression of type III collagen on immunohistochemistry (Figure 1A). This deposition became more diffuse and remarkable at 14 days in the interstitium of $Bsg^{+/+}$ mice, whereas $Bsg^{-/-}$ mice showed only a little more fibrosis. Consistent with the immunohistochemical findings, type III collagen mRNA expression also increased at 14 days in $Bsg^{+/+}$ mice compared with $Bsg^{-/-}$ mice, which was revealed by quantitative RT-PCR (Figure 1B).

PAS staining revealed marked tubular dilation and atrophy in both genotypes at 14 days (Figure 1C). It is likely that the infiltration of inflammatory cells was prominent in $Bsg^{+/+}$ mice. To verify the tubular damage, we assessed the number of dilated tubules at 7 and 14 days. There was no significant difference between the two genotypes (Figure 1D), suggesting that both groups operated on had the same extent of renal

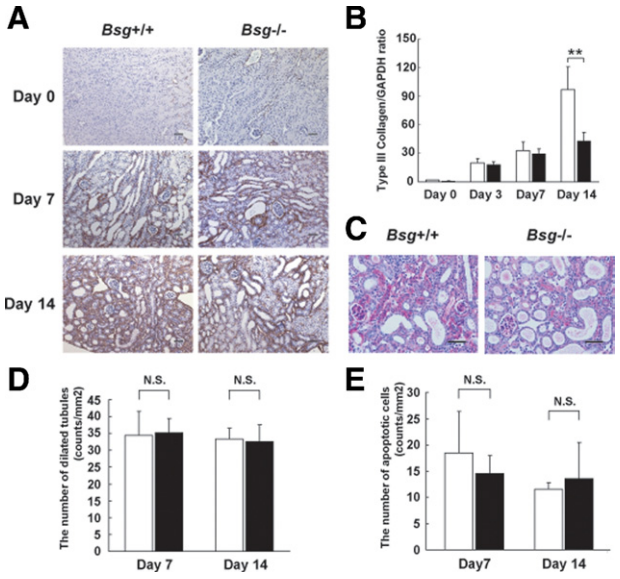

Figure 1. Histological evaluation of the kidneys of $Bsg^{+/+}$ and $Bsg^{-/-}$ mice after UUO. **A:** Type III collagen expression in the tubulointerstitium at 0, 7, and 14 days after UUO operation. Scale bar = 50 μm. **B:** Type III collagen mRNA expression, determined by quantitative reverse transcriptase PCR. Each value was standardized by GAPDH mRNA content as an internal control. Data are means (columns) ± SD (bars); white bar, $Bsg^{+/+}$; black bar, $Bsg^{-/-}$; $^{**}P < 0.01$; $n = 6$. **C:** The tubulointerstitium at 14 days is shown by PAS staining. Scale bar = 50 μm. **D:** The number of dilated tubules (counts/mm^2). Data are means ± SD; white bar, $Bsg^{+/+}$; black bar, $Bsg^{-/-}$; N.S., not significant; $n = 8$. **E:** The number of apoptotic cells (counts/mm^2), assessed by TUNEL assay. Data are means ± SD; white bar, $Bsg+/+$; black bar, $Bsg^{-/-}$; $n = 8$.

damage. We further performed TUNEL assay to examine the effect of Bsg on apoptosis of tubular injuries. But, no obvious difference was observed between the two genotypes (Figure 1E).

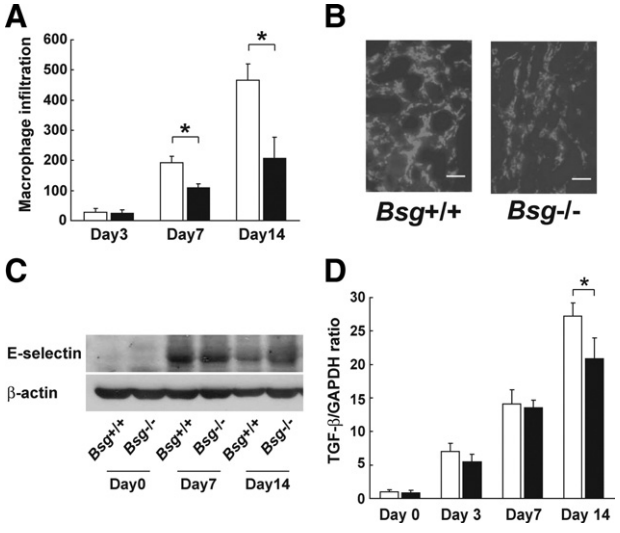

Figure 2. Macrophage infiltration in $Bsg^{+/+}$ and $Bsg^{-/-}$ mouse kidneys after UUO. **A:** The numbers of macrophages that had infiltrated into the tubulointerstitium at 3, 7, and 14 days were counted. Data are means ± SD; white bar, $Bsg^{+/+}$; black bar, $Bsg^{-/-}$; $^{*}P < 0.05$; $n = 6$. **B:** Immunofluorescence staining with F4/80 antibody at 7 days. Scale bar = 50 μm. **C:** Western blotting of E-selectin expression in the kidney after UUO. **D:** TGF-β mRNA, determined by real-time PCR. Each value was standardized by GAPDH mRNA content as an internal control. Data are means ± SD; white bar, $Bsg^{+/+}$; black bar, $Bsg^{-/-}$; $^{*}P < 0.05$; $n = 6$.

Macrophage Infiltration Is Lower in Bsg$^{-/-}$ *Mice*

Macrophage infiltration is a key event for the pathogenesis of renal fibrosis.[42,43] Both $Bsg^{+/+}$ and $Bsg^{-/-}$ mice exhibited only slight macrophage infiltration at day 3 (Figure 2A). Macrophage infiltration into the interstitium became prominent at day 7, and increased more at day 14 (Figure 2, A and B). The infiltrating macrophage number was significantly higher in the $Bsg^{+/+}$ kidneys (Figure 2A).

Macrophage infiltration in the post-obstructed kidney requires adhesion molecules.[44] However, little information about E-selectin is available. Because Bsg acts as an E-selectin ligand on inflammatory cells,[34] we next examined E-selectin expression in the kidney. We found that E-selectin expression was upregulated in the kidney after UUO surgery, but the expression levels were comparable between the genotypes (Figure 2C).

TGF-β serves as a profibrogenic cytokine by directly stimulating the synthesis of extracellular matrix components and indirectly stimulating other profibrogenic factors such as connective tissue growth factor.[45] TGF-β is produced by many types of cells in the UUO model, and

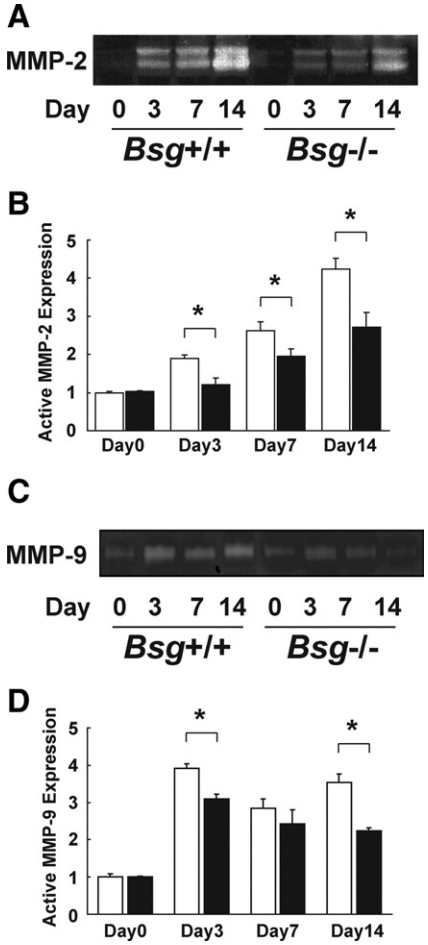

Figure 3. Induction of renal MMPs in the $Bsg^{+/+}$ and $Bsg^{-/-}$ mouse kidneys after UUO. **A:** Zymographic analysis of whole kidney lysates indicating MMP-2 induction. **B:** The intensity of active-MMP-2 bands. Data are means ± SD; white bar, $Bsg^{+/+}$; black bar, $Bsg^{-/-}$; $^{*}P < 0.05$; $n = 6$. **C:** A representative photo of MMP-9 activation in gelatin zymography. **D:** The intensity of active-MMP-9 bands. Data are means ± SD; white bar, $Bsg^{+/+}$; black bar, $Bsg^{-/-}$; $^{*}P < 0.05$; $n = 6$.

macrophage is one of the major sources.[42,45] We found that TGF-β was equally up-regulated in both genotypes until 7 days after UUO surgery (Figure 2D). Then TGF-β expression in *Bsg*$^{+/+}$ exceeded that in *Bsg*$^{-/-}$ mice at day 14 (Figure 2D).

MMP-2 and MMP-9 Activities Are Suppressed in Bsg$^{-/-}$ *Mice*

Bsg is known as an inducer of MMP-2 and MMP-9, and they play a key role in maintaining a balance between ECM deposition and degradation. In addition, the increased synthesis of MMPs has been shown to increase in various kidney diseases.[46,47] Therefore, we next investigated MMP activity in the kidney after UUO. Gelatin zymography demonstrated that the activity of MMP-2 was gradually increased, but was always less in *Bsg*$^{-/-}$ mice: the difference between the genotypes became apparent 3 days after surgery (Figure 3, A and B). On the other hand, the activation of MMP-9 strikingly increased at 3 days after UUO operation in both genotypes, but to lower extents in *Bsg*$^{-/-}$ mice at 3 days and 14 days (Figure 3, C and D). Their induction remained higher until 14 days in both groups.

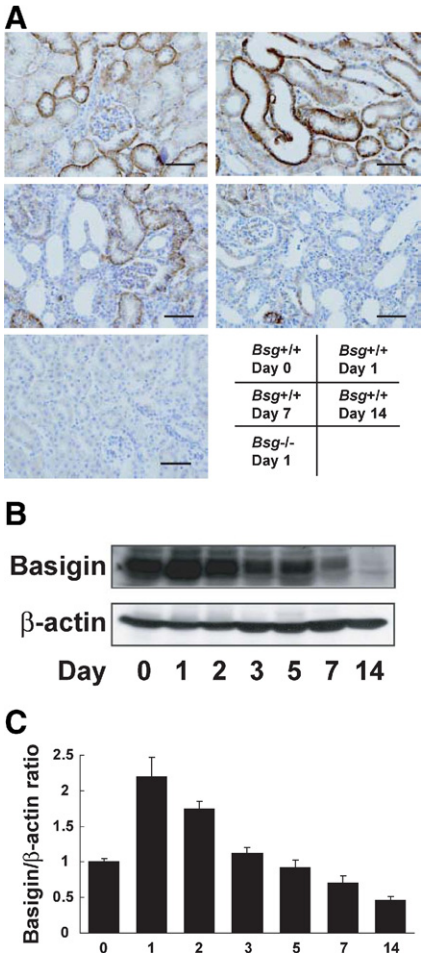

Figure 4. Basigin expression in the UUO model. **A:** Immunohistochemical staining of Bsg in the kidney. Scale bar = 50 μm. **B:** Time course of basigin expression in the UUO model. Bsg protein was determined by Western blotting. **C:** The intensity of Bsg bands was normalized as to β-actin. Data are means ± SD; $^{*}P < 0.05$; $n = 6$.

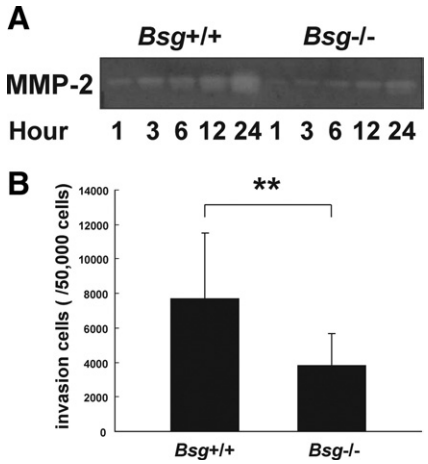

Figure 5. Bsg on TECs contributed to MMP-2 induction and upregulated migration capacity under TGF-β stimuli. **A:** Zymographic analysis indicates MMP-2 production in the culture medium of tubular epithelial cells after TGF-β stimulation. **B:** Migration of tubular epithelial cells was evaluated by cell invasion assay. The number of tubular epithelial cells that had migrated into the lower chamber through basement extract-extracts coated membrane by TGF-β stimulation is indicated. Data are means ± SD; $^{**}P < 0.01$; $n = 30$.

Bsg Expression Is Transiently Upregulated During Acute Phase of Tubulointerstitial Injury

We next examined Bsg expression during the pathogenesis of renal fibrosis. Bsg expression was detected on the basolateral side of the proximal and distal tubules in *Bsg*$^{+/+}$ mice before UUO operation (Figure 4A), consistent with a previous report.[48] UUO operation transiently and slightly enhanced Bsg expression, reaching the maximum level at day 1 (Figure 4A). However, Bsg expression decreased thereafter, and became very low at day 14 (Figure 4A). Bsg expression was detected in tubular epithelial cells and infiltrating inflammatory cells. The expression reduction was probably attributable to a loss of tubular epithelial cells due to cell death induced by UUO. Western blot data confirmed this observation (Figure 4, B and C). We did not observe any Bsg expression in the kidney of *Bsg*$^{-/-}$ mice (Figure 4A).

TGF-β Response Is Lower in Primary Bsg$^{-/-}$ *TECs*

Our *in vivo* data showed an apparent association between Bsg and renal fibrosis induced by UUO. To understand the underlying mechanism, we performed *in vitro* experiments. Based on the results shown in Figures 2 and 3, we addressed the effects of Bsg of TECs on MMP-2 production under TGF-β stimulation *in vitro*. When subjected to gelatin zymography, culture media showed that MMP-2 production was indeed induced on TGF-β administration, but the extent of the induction was much lower in *Bsg*$^{-/-}$ TECs (Figure 5A).

We also examined the invasive capacity of *Bsg*$^{+/+}$ and *Bsg*$^{-/-}$ TECs. In the upper chamber, transwell mem-

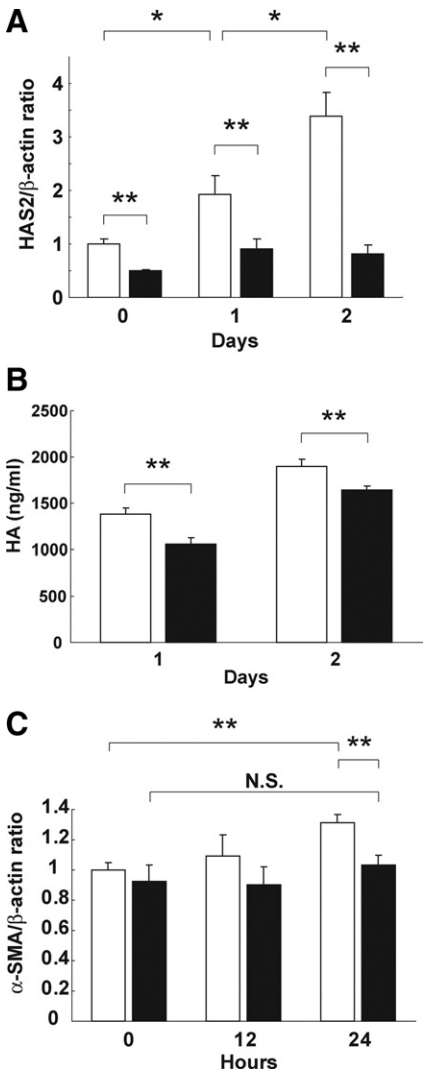

Figure 6. Bsg promoted hyaluronan synthesis and was related to α-SMA induction. **A:** Hyaluronic acid synthase 2 (HAS2) mRNA determined by real-time PCR in MEF under TGF-β stimulation. Each value was standardized by β-actin mRNA content as an internal control. Data are means ± SD; white bar, $Bsg^{+/+}$; black bar, $Bsg^{-/-}$; $^{*}P < 0.05$; $^{**}P < 0.01$; $n = 3$. **B:** Hyaluronan (HA) production in MEF under TGF-β stimulation. White bar, $Bsg^{+/+}$; black bar, $Bsg^{-/-}$; $^{**}P < 0.01$. **C:** α-SMA mRNA determined by real-time PCR in MEF under TGF-β stimuli. Each value was standardized by β-actin mRNA content as an internal control. Data are means ± SD; white bar, $Bsg^{+/+}$; black bar, $Bsg^{-/-}$; $^{**}P < 0.01$; N.S., not significant; $n = 3$.

branes were coated with basement membrane extract, and then TECs were seeded on the membrane. TGF-β was added in the lower chamber. As shown in Figure 5B, $Bsg^{-/-}$ TECs exhibited a lower ability to transmigrate.

Bsg Contributes to Hyaluronan Synthesis on TGF-β Stimulation

Because it has been reported that Bsg promotes hyaluronan production in tumor cells and fibroblasts,[23–25,49] we asked whether or not Bsg deficiency would affect hyaluronan production by MEF. We found that the expression of hyaluronic acid synthase 2, which biosynthesizes hyaluronan, was lower in $Bsg^{-/-}$ MEF even in the steady state (Figure 6A). Furthermore, TGF-β enhanced hyaluronic acid synthase 2 expression in $Bsg^{+/+}$ MEF, but not in $Bsg^{-/-}$ MEF (Figure 6A). We also found the α-SMA mRNA level was elevated 24 hours after TGF-β stimulation in $Bsg^{+/+}$ MEF, but not in $Bsg^{-/-}$ MEF (Figure 6C). This result was in line with recent reports that endogenous hyaluronan promotes α-SMA expression in fibroblast.[10,11]

Discussion

Our *in vivo* data showed that $Bsg^{-/-}$ mice had much less fibrosis, and the difference between the genotypes became apparent 14 days after UUO surgery. MMP-2 and MMP-9 activations were enhanced in both genotypes, but the extent was significantly less in $Bsg^{-/-}$ mice—the difference became apparent as early as 3 days after UUO operation. *In vitro* experiments demonstrated that Bsg on TECs promoted active MMP-2 production in response to TGF-β, and that Bsg on fibroblasts played a critic al role in hyaluronan production in response to TGF-β. Because TGF-β expression was upregulated after UUO to similar extents in $Bsg^{+/+}$ and $Bsg^{-/-}$ mice up to day 7, it is conceivable that the responsiveness to TGF-β is linked to the difference in renal fibrosis in $Bsg^{+/+}$ and $Bsg^{-/-}$ mice. In this context, it is noteworthy that both MMP-2 and MMP-9 are an activator of TGF-β,[4,5] and that Bsg is a strong inducer of MMP family. Thus, there may be a molecular circuit between Bsg, MMPs, and TGF-β (Figure 7). Taken together, our results established that Bsg is an important regulator of renal fibrosis.

UUO is a well-characterized model of renal injury leading to renal fibrosis.[43,50] A number of studies have revealed major pathways leading to the development of renal fibrosis after UUO surgery: the initial event is interstitial infiltration of macrophages that produce cytokines responsible for fibroblast proliferation and activation. After UUO operation, macrophages infiltrate the tubulointerstitial space from blood vessels and become a major source of cytokines, such as TGF-β. Macrophage infiltration was more prominent in $Bsg^{+/+}$ kidneys, and its time course was consistent with the pathogenesis profile of renal fibrosis. It is known that macrophages express Bsg, and that Bsg could be a ligand for E-selectin.[27,34] We also confirmed that Bsg on THP-1, the human monocytic cell line, bound to E-selectin (data not shown). Consider-

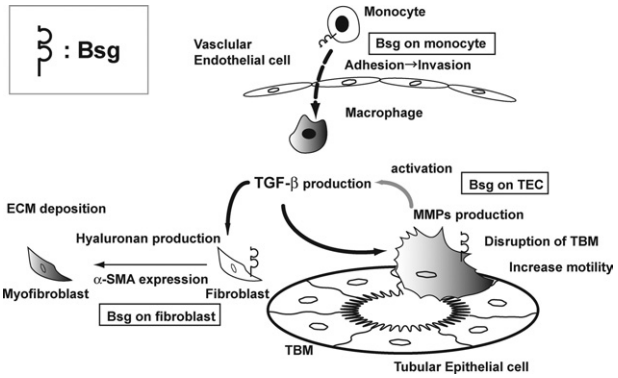

Figure 7. Schematic diagram showing the possible contribution of Bsg to renal fibrosis after UUO.

ing that E-selectin expression was induced to similar degrees in both genotypes, it is likely that the difference in macrophage infiltration between $Bsg^{+/+}$ and $Bsg^{-/-}$ mice is due to the presence of Bsg on macrophages. Indeed, it was reported that mice with triple knockout of E-, P-, and L-selectin show a marked reduction in macrophage infiltration into the obstructed kidney, and are protected from fibrosis in UUO.[51] Thus, macrophage infiltration could be the primary cause of renal fibrosis after UUO, and could cause the difference between $Bsg^{+/+}$ and $Bsg^{-/-}$ mice. In the current study, however, macrophage infiltration began 7 days after surgery, when MMP-2 expression had already been induced (starting from day 3, when TGF-β expression induction was also observed). Therefore, macrophage infiltration cannot fully explain the Bsg involvement with renal fibrosis. Moreover, TGF-β expression was induced to similar extents until 7 days in both genotypes. Our *in vitro* study demonstrated the genotype-dependent responsiveness to TGF-β in TECs and fibroblasts. Together, it is likely that both the Bsg-mediated migration of macrophages and the genotype-dependent responsiveness to TGF-β could be important to the formation of the genotype-dependent difference of renal fibrosis after UUO.

Phenotypic transition of resident renal cells into myofibroblasts is observed in a UUO model. TECs are one of them. Currently, the degree to which this process contributes to kidney fibrosis remains a matter of intense debate.[52,53] Tubular basement membrane regulates numerous cell-matrix interactions that are pivotal to the maintenance of the epithelial phenotype. In the process of renal fibrosis, MMPs are an important factor for the disruption of tubular basement membrane.[54,55] As a result, TECs lose their polarity and acquire contractile motility.[55] Considering that TECs have a TGF-β receptor and produce MMP-2 and MMP-9 on TGF-β stimulation,[56] our data suggest that Bsg on TECs (an inducer of both MMP-2 and MMP-9) is at least partly responsible for disrupting tubular basement membrane and matrix remodeling by MMP induction.

Resident fibroblasts could also be the source of myofibroblasts.[42] Generally, the wound repair process is characterized by the activation of quiescent fibroblasts and their differentiation into myofibroblasts.[30] Hyaluronan promotes α-SMA expression in fibroblasts and orchestrates TGF-β-dependent maintenance of the myofibroblast phenotype.[10,11] Little is known about the precise mechanism underlying how hyaluronan induces α-SMA in fibroblasts, but it is assumed that the hyaluronan macromolecular assembly in the pericellular environment contributes to mediate various signaling.[10] Previous reports and the present study have demonstrated that Bsg promotes hyaluronan production and subsequent α-SMA expression in fibroblasts.[25,49]

In summary, Bsg is a multifunctional molecule engaged in hyaluronan production, MMP production, cell adhesion, and α-SMA induction in renal fibrosis. Intervention targeting Bsg would have multiple effects on the prevention of renal fibrosis.

Acknowledgments

We thank Norihiko Suzuki, Naoko Asano, and Yuriko Sawa for their excellent technical assistance and Hitomi Aoyama for secretarial assistance.

References

1. Schainuck LI, Striker GE, Cutler RE, Benditt EP: Structural-functional correlations in renal disease. II. The correlations. Hum Pathol 1970, 1:631–641
2. Gabbiani G: The myofibroblast in wound healing and fibrocontractive diseases. J Pathol 2003, 200:500–503
3. Mauviel A, Chung KY, Agarwal A, Tamai K, Uitto J: Cell-specific induction of distinct oncogenes of the Jun family is responsible for differential regulation of collagenase gene expression by transforming growth factor-beta in fibroblasts and keratinocytes. J Biol Chem 1996, 271:10917–10923
4. Philipp K, Riedel F, Germann G, Hormann K, Sauerbier M: TGF-beta antisense oligonucleotides reduce mRNA expression of matrix metalloproteinases in cultured wound-healing-related cells. Int J Mol Med 2005, 15:299–303
5. Karsdal MA, Larsen L, Engsig MT, Lou H, Ferreras M, Lochter A, Delaisse JM, Foged NT: Matrix metalloproteinase-dependent activation of latent transforming growth factor-beta controls the conversion of osteoblasts into osteocytes by blocking osteoblast apoptosis. J Biol Chem 2002, 277:44061–44067
6. Yu Q, Stamenkovic I: Cell surface-localized matrix metalloproteinase-9 proteolytically activates TGF-beta and promotes tumor invasion and angiogenesis. Genes Dev 2000, 14:163–176
7. Jenkins RH, Thomas GJ, Williams JD, Steadman R: Myofibroblastic differentiation leads to hyaluronan accumulation through reduced hyaluronan turnover. J Biol Chem 2004, 279:41453–41460
8. Meran S, Thomas D, Stephens P, Martin J, Bowen T, Phillips A, Steadman R: Involvement of hyaluronan in regulation of fibroblast phenotype. J Biol Chem 2007, 282:25687–25697
9. Meran S, Thomas DW, Stephens P, Enoch S, Martin J, Steadman R, Phillips AO: Hyaluronan facilitates transforming growth factor-beta1-mediated fibroblast proliferation. J Biol Chem 2008, 283:6530–6545
10. Webber J, Jenkins RH, Meran S, Phillips A, Steadman R: Modulation of TGFbeta1-dependent myofibroblast differentiation by hyaluronan. Am J Pathol 2009, 175:148–160
11. Webber J, Meran S, Steadman R, Phillips A: Hyaluronan orchestrates transforming growth factor-beta1-dependent maintenance of myofibroblast phenotype. J Biol Chem 2009, 284:9083–9092
12. Biswas C: Tumor cell stimulation of collagenase production by fibroblasts. Biochem Biophys Res Commun 1982, 109:1026–1034
13. Yurchenko V, Constant S, Bukrinsky M: Dealing with the family: cD147 interactions with cyclophilins. Immunology 2006, 117:301–309
14. Biswas C, Zhang Y, DeCastro R, Guo H, Nakamura T, Kataoka H, Nabeshima K: The human tumor cell-derived collagenase stimulatory factor (renamed EMMPRIN) is a member of the immunoglobulin superfamily. Cancer Res 1995, 55:434–439
15. Riethdorf S, Reimers N, Assmann V, Kornfeld JW, Terracciano L, Sauter G, Pantel K: High incidence of EMMPRIN expression in human tumors. Int J Cancer 2006, 119:1800–1810
16. Schneiderhan W, Scheler M, Holzmann KH, Marx M, Gschwend JE, Bucholz M, Gress TM, Seufferlein T, Adler G, Oswald F: CD147 silencing inhibits lactate transport and reduces malignant potential of pancreatic cancer cells in in vivo and in vitro models. Gut 2009, 58:1391–1398
17. Slomiany MG, Grass GD, Robertson AD, Yang XY, Maria BL, Beeson C, Toole BP: Hyaluronan. CD44, and EMMPRIN regulate lactate efflux and membrane localization of monocarboxylate transporters in human breast carcinoma cells. Cancer Res 2009, 69:1293–1301
18. Chen X, Lin J, Kanekura T, Su J, Lin W, Xie H, Wu Y, Li J, Chen M, Chang J: A small interfering CD147-targeting RNA inhibited the proliferation, invasiveness, and metastatic activity of malignant melanoma. Cancer Res 2006, 66:11323–11330
19. Su J, Chen X, Kanekura T: A CD147-targeting siRNA inhibits the proliferation, invasiveness, and VEGF production of human malignant

melanoma cells by down-regulating glycolysis. Cancer Lett 2009, 273:140–147
20. Tang Y, Kesavan P, Nakada MT, Yan L: Tumor-stroma interaction: positive feedback regulation of extracellular matrix metalloproteinase inducer (EMMPRIN) expression and matrix metalloproteinase-dependent generation of soluble EMMPRIN. Mol Cancer Res 2004, 2:73–80
21. Tang Y, Nakada MT, Kesavan P, McCabe F, Millar H, Rafferty P, Bugelski P, Yan L: Extracellular matrix metalloproteinase inducer stimulates tumor angiogenesis by elevating vascular endothelial cell growth factor and matrix metalloproteinases. Cancer Res 2005, 65: 3193–3199
22. Tang Y, Nakada MT, Rafferty P, Laraio J, McCabe FL, Millar H, Cunningham M, Snyder LA, Bugelski P, Yan L: Regulation of vascular endothelial growth factor expression by EMMPRIN via the PI3K-Akt signaling pathway. Mol Cancer Res 2006, 4:371–377
23. Misra S, Ghatak S, Zoltan-Jones A, Toole BP: Regulation of multidrug resistance in cancer cells by hyaluronan. J Biol Chem 2003, 278: 25285–25288
24. Marieb EA, Zoltan-Jones A, Li R, Misra S, Ghatak S, Cao J, Zucker S, Toole BP: Emmprin promotes anchorage-independent growth in human mammary carcinoma cells by stimulating hyaluronan production. Cancer Res 2004, 64:1229–1232
25. Toole BP: Hyaluronan: from extracellular glue to pericellular cue. Nat Rev Cancer 2004, 4:528–539
26. Tang W, Chang SB, Hemler ME: Links between CD147 function, glycosylation, and caveolin-1. Mol Biol Cell 2004, 15:4043–4050
27. Arora K, Gwinn WM, Bower MA, Watson A, Okwumabua I, MacDonald HR, Bukrinsky MI, Constant SL: Extracellular cyclophilins contribute to the regulation of inflammatory responses. J Immunol 2005, 175:517–522
28. Kirk P, Wilson MC, Heddle C, Brown MH, Barclay AN, Halestrap AP: CD147 is tightly associated with lactate transporters MCT1 and MCT4 and facilitates their cell surface expression. EMBO J 2000, 19:3896–3904
29. Philp NJ, Wang D, Yoon H, Hjelmeland LM: Polarized expression of monocarboxylate transporters in human retinal pigment epithelium and ARPE-19 cells. Invest Ophthalmol Vis Sci 2003, 44:1716–1721
30. Huet E, Vallee B, Szul D, Verrecchia F, Mourah S, Jester JV, Hoang-Xuan T, Menashi S, Gabison EE: Extracellular matrix metalloproteinase inducer/CD147 promotes myofibroblast differentiation by inducing alpha-smooth muscle actin expression and collagen gel contraction: implications in tissue remodeling. FASEB J 2008, 22: 1144–1154
31. Igakura T, Kadomatsu K, Kaname T, Muramatsu H, Fan QW, Miyauchi T, Toyama Y, Kuno N, Yuasa S, Takahashi M, Senda T, Taguchi O, Yamamura K, Arimura K, Muramatsu T: A null mutation in basigin, an immunoglobulin superfamily member, indicates its important roles in peri-implantation development and spermatogenesis. Dev Biol 1998, 194:152–165
32. Igakura T, Kadomatsu K, Taguchi O, Muramatsu H, Kaname T, Miyauchi T, Yamamura K, Arimura K, Muramatsu T: Roles of basigin, a member of the immunoglobulin superfamily, in behavior as to an irritating odor, lymphocyte response, and blood-brain barrier. Biochem Biophys Res Commun 1996, 224:33–36
33. Naruhashi K, Kadomatsu K, Igakura T, Fan QW, Kuno N, Muramatsu H, Miyauchi T, Hasegawa T, Itoh A, Muramatsu T, Nabeshima T: Abnormalities of sensory and memory functions in mice lacking Bsg gene. Biochem Biophys Res Commun 1997, 236:733–737
34. Kato N, Yuzawa Y, Kosugi T, Hobo A, Sato W, Miwa Y, Sakamoto K, Matsuo S, Kadomatsu K: The E-selectin ligand basigin/CD147 is responsible for neutrophil recruitment in renal ischemia/reperfusion. J Am Soc Nephrol 2009, 20:1565–1576
35. Chen S, Kadomatsu K, Kondo M, Toyama Y, Toshimori K, Ueno S, Miyake Y, Muramatsu T: Effects of flanking genes on the phenotypes of mice deficient in basigin/CD147. Biochem Biophys Res Commun 2004, 324:147–153
36. Nomura A, Nishikawa K, Yuzawa Y, Okada H, Morgan BP, Piddlesden SJ, Nadai M, Hasegawa T, Matsuo S: Tubulointestinal injury induced in rats by a monoclonal antibody that inhibits function of membrane inhibitor of complement. J Clin Invest 1995, 96:2348–2356
37. Kadomatsu K, Hagihara M, Akhter S, Fan QW, Muramatsu H, Muramatsu T: Midkine induces the transformation of NIH3T3 cells. Br J Cancer 1997, 75:354–359
38. Kosugi T, Yuzawa Y, Sato W, Arata-Kawai H, Suzuki N, Kato N, Matsuo S, Kadomatsu K: Midkine is involved in tubulointerstitial inflammation associated with diabetic nephropathy. Lab Invest 2007, 87:903–913
39. Camussi G, Brentijens JR, Noble B, Kerjaschiki D, Malavasi F, Roholt OA, Farquhar MG, Andres G: Antibody-induced redistribution of Hymann antigen on the surface of cultured glomerular visceral epithelial cells: possible role in the pathogenesis of Hymann glomerulonephritis. J Immunol 1985, 135:2409–2416
40. Tsuboi N, Yoshikai Y, Matsuo S, Kikuchi T, Iwami K, Nagai Y, Takeuchi O, Akira S, Matsuguchi T: Roles of toll-like receptors in C-C chemokine production by renal epithelial cells. J Immunol 2002, 169:2026–2033
41. Nguyen A, Burack WR, Stock JL, Kortum R, Chaika OV, Afkarian M, Muller WJ, Murphy KM, Morrison DK, Lewis RE, McNeish J, Shaw AS: Kinase suppressor of Ras (KSR) is a scaffold which facilitates mitogen-activated protein kinase activation in vivo. Mol Cell Biol 2002, 22:3035–3045
42. Chevalier RL, Forbes MS, Thornhill BA: Ureteral obstruction as a model of renal interstitial fibrosis and obstructive nephropathy. Kidney Int 2009, 75:1145–1152
43. Bascands JL, Schanstra JP: Obstructive nephropathy: insights from genetically engineered animals. Kidney Int 2005, 68:925–937
44. Rouschop KM, Sewnath ME, Claessen N, Roelofs JJ, Hoedemaeker I, van der Neut R, Aten J, Pals ST, Weening JJ, Florquin S: CD44 deficiency increases tubular damage but reduces renal fibrosis in obstructive nephropathy. J Am Soc Nephrol 2004, 15:674–686
45. Wolf G: Renal injury due to renin-angiotensin-aldosterone system activation of the transforming growth factor-beta pathway. Kidney Int 2006, 70:1914–1919
46. Steinmann-Niggli K, Ziswiler R, Kung M, Marti HP: Inhibition of matrix metalloproteinases attenuates anti-Thy1.1 nephritis. J Am Soc Nephrol 1998, 9:397–407
47. Marti HP, McNeil L, Thomas G, Davies M, Lovett DH: Molecular characterization of a low-molecular-mass matrix metalloproteinase secreted by glomerular mesangial cells as PUMP-1. Biochem J 1992, 285(Pt 3):899–905
48. Deora AA, Philp N, Hu J, Bok D, Rodriguez-Boulan E: Mechanisms regulating tissue-specific polarity of monocarboxylate transporters and their chaperone CD147 in kidney and retinal epithelia. Proc Natl Acad Sci U S A 2005, 102:16245–16250
49. Toole BP, Slomiany MG: Hyaluronan. CD44 and Emmprin: partners in cancer cell chemoresistance. Drug Resist Updat 2008, 11:110–121
50. Klahr S, Morrissey J: Obstructive nephropathy and renal fibrosis. Am J Physiol Renal Physiol 2002, 283:F861–875
51. Lange-Sperandio B, Cachat F, Thornhill BA, Chevalier RL: Selectins mediate macrophage infiltration in obstructive nephropathy in newborn mice. Kidney Int 2002, 61:516–524
52. Lin SL, Kisseleva T, Brenner DA, Duffield JS: Pericytes and perivascular fibroblasts are the primary source of collagen-producing cells in obstructive fibrosis of the kidney. Am J Pathol 2008, 173:1617–1627
53. Liu Y: New insights into epithelial-mesenchymal transition in kidney fibrosis. J Am Soc Nephrol 2010, 21:212–222
54. Zavadil J, Bottinger EP: TGF-beta and epithelial-to-mesenchymal transitions. Oncogene 2005, 24:5764–5774
55. Zeisberg M, Maeshima Y, Mosterman B, Kalluri R: Renal fibrosis. Extracellular matrix microenvironment regulates migratory behavior of activated tubular epithelial cells. Am J Pathol 2002, 160:2001–2008
56. Yang J, Liu Y: Dissection of key events in tubular epithelial to myofibroblast transition and its implications in renal interstitial fibrosis. Am J Pathol 2001, 159:1465–1475